Journal of Mammalogy, 2025, **106**, 187–201
https://doi.org/10.1093/jmammal/gyae085
Advance access publication 13 September 2024
Research Article

Research Article

Systematics of the *Rhinolophus landeri* complex, with evidence for 3 additional Afrotropical bat species

Bruce D. Patterson[1,*], Terrence C. Demos[1], Laura Torrent[2,3], Amanda L. Grunwald[4], Cecilia Montauban[5,6], Julian C. Kerbis Peterhans[1,7], Molly M. McDonough[1,8], Carl W. Dick[1,9], Michael Bartonjo[10], M. Corrie Schoeman[11], Luis A. Ruedas[4], Javier Juste[12,13]

[1]Negaunee Integrative Research Center, Field Museum of Natural History, 1400 S. DuSable Lake Shore Drive, Chicago, IL 60605, United States
[2]CIBIO-InBIO, Research Centre in Biodiversity and Genetic Resources, University of Porto, Campus de Vairão, 4485-661 Vairão, Portugal
[3]BiBio, Natural Sciences Museum of Granollers, Francesc Macià 51, 08402 Granollers, Spain
[4]Department of Biology and Museum of Vertebrate Biology, Portland State University, SRTC-247, P.O. Box 751, Portland, OR 97207, United States
[5]Department of Life Sciences, Imperial College London, Ascot, Berks SL5 7PY, United Kingdom
[6]Department of Life Sciences, Natural History Museum London, London SW7 5BD, United Kingdom
[7]College of Arts & Sciences, Roosevelt University, Chicago, IL 60605, United States
[8]Department of Biological Sciences, Chicago State University, 9501 S. King Drive, Chicago, IL 60628, United States
[9]Department of Biology, Western Kentucky University, Bowling Green, KY 42101, United States
[10]Mammalogy Section, National Museums of Kenya, P.O. Box 40658 – 00100, Nairobi, Kenya
[11]School of Life Sciences, University of KwaZulu-Natal, Durban 4000, South Africa
[12]Estación Biológica de Doñana (CSIC), Avda. Américo Vespucio 26, Seville 41092, Spain
[13]Epidemiology and Public Health, CIBERESP, 28029 Madrid, Spain

*Corresponding author: Negaunee Integrative Research Center, Field Museum of Natural History, 1400 S DuSable Lake Shore Drive, Chicago, IL 60605, United States. Email: bpatterson@fieldmuseum.org

Version of Record, first published online September 13, 2024, with fixed content and layout in compliance with Art. 8.1.3.2 ICZN.
Nomenclatural statement.—A Life Science Identifier (LSID) number was obtained for this publication: urn:lsid:zoobank.org:pub:25A48F5E-3C37-4A82-8442-08EFEFAF115F
Associate Editor was Michael McGowen

Abstract

Roughly a third of all horseshoe bat species (Rhinolophidae: *Rhinolophus*) are found in Africa, where a recent continent-wide genetic survey suggested the presence of both undescribed and apparently invalid species. Here, we focus on the *R. landeri* species complex and the recent elevation of *R. lobatus* Peters, 1852, to species rank. That action created ambiguity in the taxonomy of East African members of the group—are both *R. landeri* Martin, 1838, and *R. lobatus* sympatric in East Africa or is another, unnamed species present there? Here, we refine genetic, morphological, and behavioral characterizations of *R. landeri* and its erstwhile synonyms with samples from the vicinity of their type localities. The distribution of *R. landeri* appears to be limited to Central and West Africa; existing genetic records attributed to this species from Mali clearly represent another taxon. We marshal genetic evidence for the species-level distinction of *R. dobsoni* Thomas, 1904, from Sudan, which was previously considered a synonym of *R. landeri*. We reject *R. axillaris* J. A. Allen, 1917, as a synonym of the *R. landeri* complex, provisionally regarding it as a valid member of the *landeri* species group. Finally, we demonstrate that East Africa is home to a fourth species of the *landeri* complex that is named herein. Final resolution of the systematics of this species complex awaits expanded characterizations (especially of genetics, vocalizations, and noseleaves) and studies of variation in regions of contact.

Key words: Afrotropical, Chiroptera, genetics, Rhinolophidae, species complex, systematics, vocalizations.

The bat genus *Rhinolophus*, sole extant member of the Rhinolophidae (horseshoe bats), includes aerial insectivores distributed over most of the tropical, subtropical, and temperate regions of Africa, Eurasia, Oceania, and Australasia. The group originated in Asia (Guillen Servent et al. 2003; Chornelia and Hughes 2022), with a single colonization giving rise to a clade of African and Palearctic species (Dool et al. 2016; Demos et al. 2019). With 112 recognized species, *Rhinolophus* is now the third most speciose genus of mammals, trailing only *Crocidura* and *Myotis* (Mammal Diversity Database 2023). Remarkably, a third of all recognized *Rhinolophus* species have been discovered (or rediscovered) in the last 2 decades (cf. Simmons 2005). Genetic and echolocation call analyses have contributed importantly to our enhanced understanding of diversity in this and other insectivorous bat families (e.g., Tu et al. 2017; Mao et al. 2019; Srinivasulu et al. 2019).

Phylogenetic analyses consistently recover the *R. landeri* species group (Csorba et al. 2003) as the earliest diverging group in the African–Palearctic clade (Dool et al. 2016; Demos et al. 2019). The group currently includes 4 Afrotropical endemics: *R. landeri* W. Martin, 1838—once thought to be continentally distributed (e.g.,

Received: March 5, 2024; Editorial Decision: July 9, 2024; Accepted: July 29, 2024

Happold 2013b) but now used for populations in West and Central Africa; *R. lobatus* Peters, 1852—formerly treated as a subspecies of *R. landeri*, but now regarded as distinct in Southern and Eastern Africa (Taylor et al. 2018, 2019); *R. alcyone* Temminck, 1853—distributed in equatorial West and Central African rainforests; and *R. guineensis* Eisentraut, 1960—with a range restricted to far West Africa (Fig. 1). Formerly, the group also included *Rhinolophus blasii* Peters, 1867, which can now be confidently placed in the *euryale* species group (Dool et al. 2016; Demos et al. 2019; Bücs and Csorba 2022). The *landeri* species group is distinguished from other *Rhinolophus* species groups by a wedge-shaped sella, triangular connecting process, and the presence of axillary tufts in the armpits of some males (Csorba et al. 2003).

Rhinolophus alcyone is much larger than the remaining 3 species (forearm length [FA] 49 to 56 mm) and *R. guineensis* (FA 44 to 50 mm) is generally larger than *R. landeri* (FA 35 to 49 mm) where the 2 are sympatric; additionally, *R. guineensis* has whitish (not rusty) axillary tufts (Rosevear 1965; Koopman 1989; Happold 2013a). Notably, neither *R. alcyone* nor *R. guineensis* has junior synonyms. On the other hand, the species *R. landeri* and *R. lobatus* are same-sized and geographically variable; these 2 taxa and their synonyms are here termed the *landeri* complex with reference to the extended synonymy of *lobatus* within *landeri*. Mammal Diversity Database (2023) lists 3 taxa in the synonymy of *R. landeri*: *landeri*, *dobsoni* Thomas, 1904, and *axillaris* J. A. Allen, 1917. *Rhinolophus landeri* is thought to range from Senegal and Gambia in West Africa into Central Africa, as far north as Sudan and as far east as Ethiopia and Kenya. Its type locality is "Insulâ Fernando Po [= Bioko Island]," Equatorial Guinea. Mammal Diversity Database (2023) lists 2 taxa in the synonymy of *Rhinolophus lobatus*: *lobatus* Peters, 1852 and *angolensis* Seabra, 1898. The latter is very poorly known, has never been revised, and is listed in the synonymy of *R. landeri* by Simmons and Cirranello (2024) and in that of *R. lobatus* by Beja et al. (2019). *Rhinolophus lobatus* is currently thought to range over Eastern and Southern Africa, from South Sudan and Kenya to Angola and South Africa (Taylor et al. 2018; mol.org). Peters (1852) gave its type locality as "Africa orientalis, Sena, Tette, 17° Aust.," Mozambique, but this was subsequently restricted to Sena, Mozambique by Moreau et al. (1946).

The validity and limits of taxa in the *landeri* complex—that is, *R. landeri*, *R. lobatus*, and their synonyms—have been uncertain since the first generic revision. In reviewing this group, Anderson (1906:189) stated "*Rh. landeri* and *lobatus* are very closely related. *Rh. landeri* has a shorter tibia and tail; the skull is rather more slender than, but in other respects quite similar to, that of *lobatus*; the dentition is the same. It is not unlikely that, when a completer material is to hand, we shall have to regard *Rh. landeri* and *lobatus* as western and eastern representatives of 1 species. As to *Rh. dobsoni*, from Kordofan, I have some doubt that it is distinguishable from *Rh. lobatus*; but... I prefer for the present to leave the question open." Confusion continues today with the distributions of both *R. landeri* and *R. lobatus* thought to overlap broadly in East Africa (e.g., mol.org). However, genetic surveys strongly suggest that neither species actually occurs in Kenya and that a different species may be involved (bats identified as "cf. *landeri*" in Demos et al. 2019).

Therefore, the goals of our study were to characterize more thoroughly the valid taxa in the *R. landeri* complex in terms of their genetics, craniometrics, and echolocation calls. We also sought to determine which if any of the available names applies to a well-supported clade of bats from Kenya uncovered in recent genetic surveys (Demos et al. 2019). The resulting characterizations and distinctions between taxa should enable more confident identifications of these *Rhinolophus* species, closer specifications of their distributions, and fuller resolution of their relationships.

Materials and methods.

Selection of taxa and sampling.

Most new genetic data from tissue samples used in this study (n = 80) were obtained from specimens previously catalogued and part of the permanent collections of the following natural history museums: Field Museum of Natural History, Chicago, United States; National Museums of Kenya, Nairobi, Kenya; Mammal Collections, Estación Biológica de Doñana (CSIC), Seville, Spain; and Natural History Museum, London, United Kingdom. Ten samples from Ghana were obtained from wing punches of bats released at the point of capture (Fig. 1). Where possible, specimens were obtained from localities close to the type localities of taxa in the *landeri* species complex, including *landeri* from Bioko Island, *dobsoni* from Sudan, and *lobatus* from Mozambique. The provenance of all specimens and sequences used is listed in Supplementary Data SD1 and depicted in Fig. 1.

DNA extraction, amplification, and Sanger sequencing.

Whole-genomic DNA was extracted from 74 frozen tissue samples of *Rhinolophus* using the QIAGEN DNeasy Blood and Tissue Kit (Germantown, Maryland). An additional 112 *Rhinolophus* sequences were downloaded from GenBank (Supplementary Data SD1). Fresh specimens were sequenced for mitochondrial Cytochrome *b* (*Cytb*), using the primer pair LGL 765F and LGL 766R (Bickham et al. 1995, 2004), and 7 unlinked autosomal nuclear introns: SLC38A7 intron 8 (AAT), ABHD11 intron 5 (ABHD11), ACOX2 intron 3 (ACOX2), ACPT intron 4 (ACPT), COPS7A intron 4 (COPS7A), ROGDI intron 7 (ROGDI), and STAT5A intron 16 (STAT5A; Mathee et al. 2001; Igea et al. 2010; Salicini et al. 2011). PCR (polymerase chain reaction) amplifications were carried out using the same thermocycler protocols as in Demos et al. (2018). Amplified PCR products were purified using ExoSAP-IT (Thermo Scientific, Waltham, Massachusetts). Sequencing was carried out in both directions on an ABI-3100 thermocycler (Applied Biosystems, Foster City, California) at the Pritzker Laboratory for Molecular Systematics and Evolution (FMNH).

In addition to the above amplification protocols for frozen tissues, 6 samples were derived from hindfoot toe clips of dried study skins (hereafter referred to as historic samples; FMNH 34164, 35381, 48714, 108154 to 108156). DNA of historic samples was extracted using the phenol–chloroform protocol as detailed in McDonough et al. (2018). DNA sample concentration was increased using Amicon Ultra-4 columns with an Ultracel 30 membrane (Millipore Sigma, Burlington, Massachusetts).

For library preparation of historical samples, DNA was not sheared and irrespective of the starting concentration, 35 µL of DNA were aliquoted and concentrated using a 3X bead clean-up using MagNA following Rohland and Reich (2012) and resuspended in 14 µL of elution buffer. Library preparation was performed using KAPA HyperPrep (Kapa Biosystems) for Illumina platforms following the manufacturer's protocol but was modified to use one-quarter of the reagents per reaction. Amplifications were performed using 15 cycles with iTru dual indexing primers and KAPA HiFi Hotstart ReadyMix (Kapa Biosystems) followed by a 1.2X bead clean-up. Library concentrations were measured with a Qubit dsDNA High Sensitivity Assay kit (Invitrogen) and pooled with other samples in equal nanomolar concentrations; sequencing was performed in the Field Museum Pritzker DNA lab using a MiSeq Illumina system.

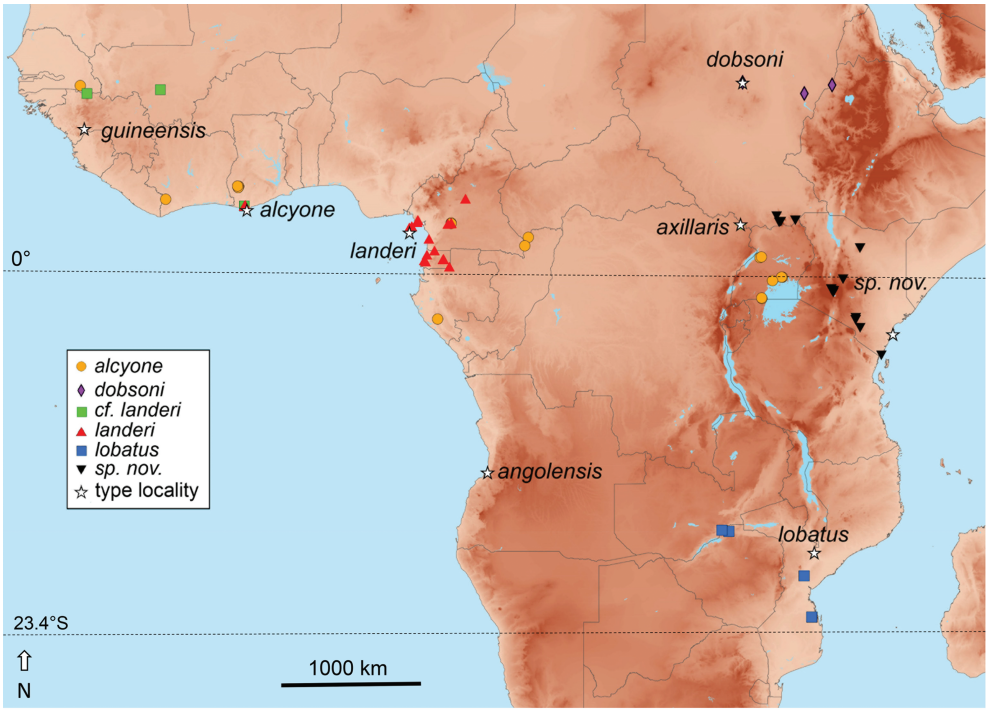

Fig. 1. Map of taxonomic and geographic sampling for study of the *Rhinolophus landeri* species group (all taxa) and the *landeri* complex (*dobsoni*, *landeri*, *lobatus*, and sp. nov.). Stars mark type localities for taxa in the *landeri* group: orange circles, *R. alcyone*; purple diamonds, *R. dobsoni*; red triangles, *R. landeri*; blue squares, *R. lobatus*; and the clade from Kenya and South Sudan, labeled sp. nov., inverted triangles. The green squares denote locations of the western *Cytb* subclade of *R. landeri*. See text for discussion.

After demultiplexing, we combined paired-end reads using FLASH2 v. 2.2.00 (Magoč and Salzberg 2011) and trimmed adapter sequences using TrimGalore v. 0.4.3 (Krueger 2017). Poor quality sequences (scores below 20) and exact PCR replicates were removed using prinseq-lite v.0.20.4 (Schmieder and Edwards 2011). Reads were then mapped to a *Rhinolophus* reference genome using the Burrows–Wheeler algorithm in BWA v.7.10 (Li and Durbin 2011) and use of the "bwa mem" command.

Gene trees and haplotype networks.

Sequences were assembled and edited using GENEIOUS PRIME v. 2023.1.1 (Biomatters Ltd). Sequences were aligned using MUSCLE with default settings in GENEIOUS. Protein coding data from *Cytb* were translated to amino acids to set codon positions and confirm the absence of premature stop codons, deletions, and insertions. Several gaps were incorporated in the alignments of the nuclear introns, but their positions were unambiguous.

Maximum likelihood (ML) estimates of *Cytb* gene trees and a concatenated alignment of the 7 partitioned introns were made using the program IQ-TREE version 2.2.2.7 (Minh et al. 2020) on the CIPRES portal. The TESTNEW option was implemented using extended model selection that included the FreeRate model and was immediately followed by tree reconstruction using the best-fit model found. We conducted analyses using the ultrafast bootstrap algorithm to search for the best-scoring ML tree algorithm with 1,000 bootstrap replicates. Horseshoe bat species belonging to other species groups (Csorba 2008; Demos et al. 2019) served as outgroups for the *landeri* species group analyses: *R. deckenii* (*ferrumequinum* group) and *R. luctus* (*trifoliatus* group) for the *Cytb* analysis and *R. damarensis* (*fumigatus* group) for the nuclear introns. PopART v. 1.7 (Leigh and Bryant 2015) was used to construct a median-joining network of *Cytb* haplotypes for populations within the *landeri* species group. Pie charts were used to visualize the relative frequencies and relationships of haplotypes in these populations. Uncorrected sequence divergences (*p*-distances) within and between species/clades were calculated for *Cytb* using MEGA X v.11.0.13 (Kumar et al. 2018). Tree files in the Nexus format are archived on Mendeley Data (DOI: 10.17632/mxgyjsj66t.1).

Morphological analyses.

We analyzed the external and craniodental morphology of 195 *R. landeri* species group members distributed in Cameroon, Central African Republic, Equatorial Guinea, Gabon, Kenya, Mozambique, South Sudan, Sudan, and Uganda (Supplementary Data SD1). Morphometric analyses centered on voucher specimens housed in 3 natural history museums: Field Museum of Natural History, Chicago, Illinois, United States (FMNH); Royal Ontario Museum, Toronto, Ontario, Canada (ROM); and Estación Biológica de Doñana, Seville, Spain (EBD). We also had access to photos and published reports of specimens from the American Museum of Natural History, New York (AMNH); Natural History Museum, London, United Kingdom (NHMUK); and the Natural History Museum, Berlin, Germany (ZMB).

We collected morphometric data only from adults, corresponding to those specimens with completely erupted and partly worn dentitions. External measurements relied on those taken by the collector and recorded on skin tags. In addition, 12 craniodental measurements—as defined and depicted by Velazco and Gardner (2012)—were taken using digital calipers at 0.01 mm resolution: GLS, greatest length of skull; CIL, condyloincisive length; CCL, condylocanine length; BB, braincase breadth; ZB, zygomatic breadth; PB, postorbital breadth; MSTW, mastoid width; MPW, mastoid

process width; MTRL, maxillary toothrow length; MLTRL, postcanine toothrow length; M2–M2, width at M2; DENL, dentary length; and MANDL, mandibular toothrow length.

Statistical analyses relied on the Statistica 7.1 package (StatSoft 2005). Group distributions were summarized by means, sample size, standard deviations, and range (minimum and maximum values). Tests for differences among taxa relied on *F*-tests implemented with the breakdown and 1-way ANOVA routine; the same routine provided post hoc tests of pairs of taxa using Tukey's HSD statistic. In all cases, $P < 0.05$ was taken as indicating a significant difference. Principal components analysis was conducted on untransformed variables using the covariance matrix. Because discriminant function analysis is sensitive to violations of homoscedasticity, log-transformed variables were used in stepwise analysis of the *landeri* complex members.

Vocalization analyses.

Echolocation calls of members of the *landeri* complex were recorded in the hand using several acoustic recorders. Bats in Kenya were recorded with bats held in the hand ca. 30 cm away from the microphone of a D1000X bat detector (Pettersson Elektronik AB, Uppsala, Sweden; www.batsound.se; 384 kHz sampling rate, 16-bit resolution). In Mozambique, *lobatus* individuals were recorded with an Avisoft Ultrasound 116Hb Bat Detector (Avisoft Bioacoustics, Berlin, Germany; 300 kHz sampling rate, 16 bits, mono, with a threshold of 16) connected to an HP Pavillion 6210 notebook (Hewlett Packard Development Company, Palo Alto, California). In Cameroon, Equatorial Guinea, and Ghana, echolocation calls were recorded using Wildlife Acoustics Echo Meter Touch 2 Pro Android (Wildlife Acoustics, Inc., Maynard, Massachusetts; Firmware Version: App 2.8.14; 384 kHz sampling rate, 16-bit resolution) on Galaxy and Samsung smartphones. All detectors used in this study are digital recorders with high sampling frequencies that offer full-spectrum recording capability and capture the full bandwidth of the call (Moir et al. 2013).

We recorded handheld bats because, without the Doppler-shift compensation associated with flight, the "resting frequency" of these stationary individuals varies very little within a sequence (Fenton et al. 2012; Hiryu et al. 2016); this makes handheld calls best suited for frequency comparisons between individuals or populations. The recorded sequences were stored as .wav files and graphically examined using the software BatSound 4.3 (Pettersson Elektronik, Uppsala, Sweden). A customized 512-point fast Fourier transform with a Hanning window was used for sound analysis, accounting for both the power spectrum and spectrograms. In accordance with Jung et al. (2014), we measured the bandwidth, call duration (ms), call interval (ms), maximum frequency (StartF) and minimum frequency (EndF), and peak frequency or frequency of maximum energy, using KaleidoScope v.3.1.4b (Wildlife Acoustics). For every bat, the mean of 10 calls with the best signal-to-noise ratios was determined and used in all analyses.

Results

Phylogenetic analyses.

Pairwise *Cytb* genetic distances among species of the *R. landeri* species group appear in Table 1. The average difference between species pairs is 5.5%, *alcyone* is most distant from the remaining species (mean 6.4%), and the closest pair is *landeri* and cf. *landeri* (3%). The clade from Kenya and South Sudan (labeled in figures and tables as sp. nov.) averages 5.7% distant from named taxa in the group and is nearest to *dobsoni* from Sudan (4.5%).

The ML tree for *Cytb* sequences of the *landeri* species group appears in Fig. 2. Each of the species *R. alcyone*, *R. landeri*, and *R. lobatus* are strongly supported in the analysis (bs = 100). In addition, the clade from Kenya and South Sudan and *dobsoni* from Sudan are each recovered as monophyletic with strong support (bs = 100), and as sisters to *landeri* (bs = 86). The latter clade contains well-supported (bs ≥ 71) subgroups from Central Africa plus Bioko Island (the type locality of *landeri*) and from far West Africa (Senegal and Mali, labeled as cf. *landeri*); members of both groups are present in Ghana. There is moderate support (bs = 65) for *lobatus* as sister to the remainder of the *landeri* complex, and strong support (bs = 100) for *alcyone* being sister to the *landeri* complex as a whole. *R. alcyone* also contains well-supported subgroups from Central and West Africa.

A substitution network of the *Cytb* haplotypes appears in Fig. 3. No haplotype is shared among taxa. Most haplotypes are strongly regional and limited to a single country, exceptions being a *lobatus* haplotype in both Mozambique and neighboring Zimbabwe and an *alcyone* haplotype found both in Gabon and Central African Republic. At least 10 *Cytb* substitutions separate all members of the *landeri* species group from each other. As in the ML tree, *lobatus*, *dobsoni*, and the clade from Kenya and South Sudan are each homogeneous and well distinguished from others, exhibiting a star-like structure; on the other hand, *alcyone* and *landeri* contain more heterogeneous, geographically structured haplotypes, perhaps reflecting their broader geographic sampling.

The 7 nuclear introns yield a different topology and offer varying support for these groupings (Fig. 4). Neither *landeri* nor *lobatus* is recovered as reciprocally monophyletic in the ML intron tree. However, there is strong support (bs > 97) for the monophyly of both *alcyone* and the clade from Kenya and South Sudan. Curiously, sequences of cf. *landeri* from SAN 95 and SAN 96, which were strongly supported as sister to the Central African *landeri* clade in the *Cytb* analysis, are recovered in the intron analysis as lying outside all surveyed members of the *landeri* species group.

Morphometric analyses.

External characters of the *R. landeri* species group are presented in Table 2; also included are analyses of variance among members of the *landeri* complex. The substantially larger size of *R. alcyone* is immediately apparent and is the rationale for limiting ANOVAs to members of the *landeri* complex. Half of the variables show significant variation among the 4 taxa including TL, HF, and FA, but mean differences are small and overlapping ranges are appreciable.

Craniodental variables for the *landeri* species group are presented in Table 3. As with external variables, *R. alcyone* is far larger than the remaining taxa. Just over half (57%) of the variables vary significantly among members of the *landeri* complex, but again differences

Table 1. Number of base differences per site, averaged among 121 nucleotide sequences over 1,140 base positions of *Cytb*. Boldfaced entries on diagonal measure intraspecific variation in our samples.

	alcyone	*dobsoni*	*landeri*	cf. *landeri*	*lobatus*	sp. nov.
alcyone	**0.017**					
dobsoni	0.063	**0.007**				
landeri	0.065	0.053	**0.009**			
cf. *landeri*	0.062	0.050	0.030	**0.015**		
lobatus	0.061	0.056	0.057	0.050	**0.002**	
sp. nov.	0.067	0.045	0.058	0.057	0.058	**0.003**

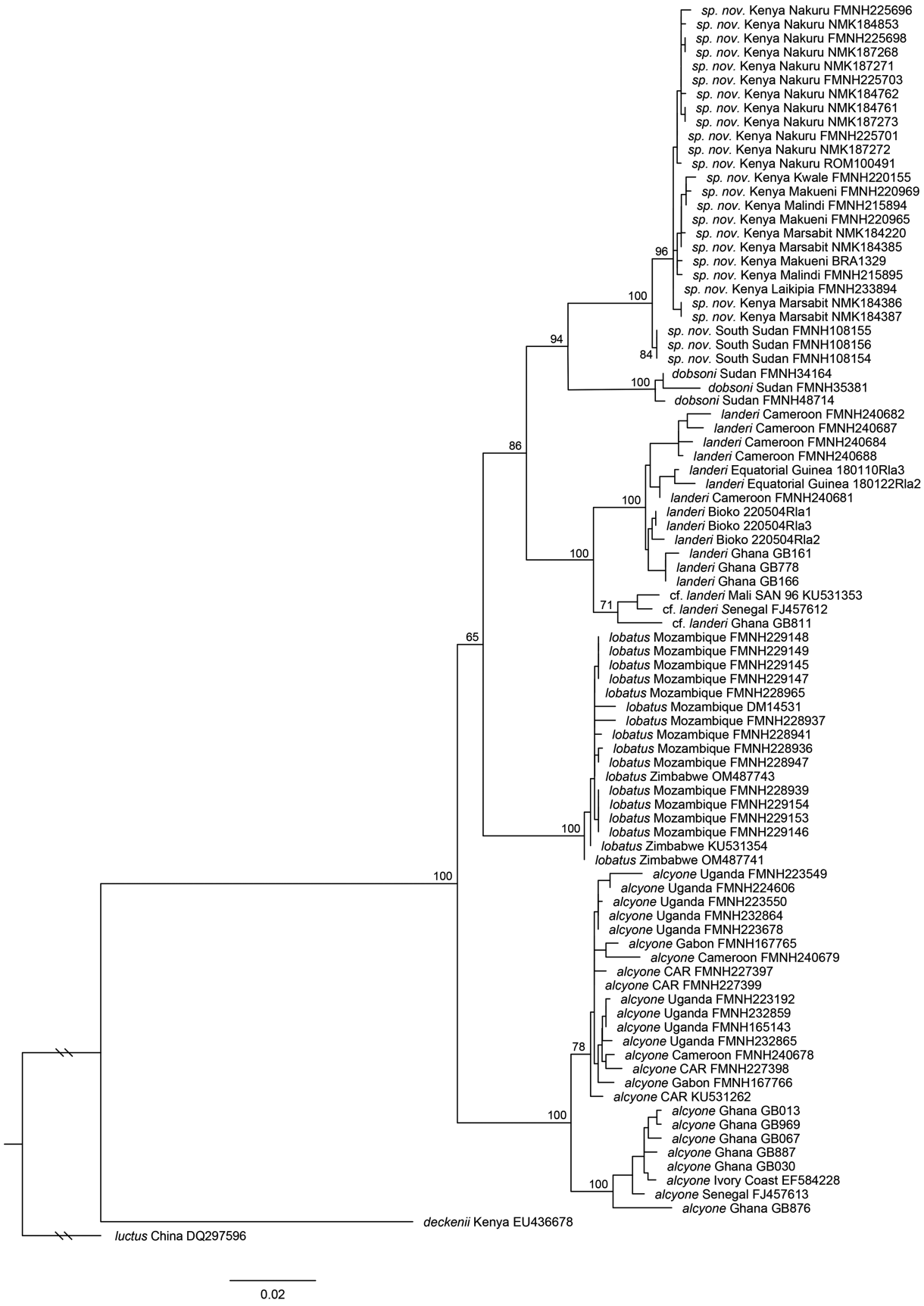

Fig. 2. Maximum likelihood phylogeny of mitochondrial *Cytb* sequences of the *Rhinolophus landeri* species group. The phylogeny was inferred in IQ-TREE. Bootstrap values are included at major nodes.

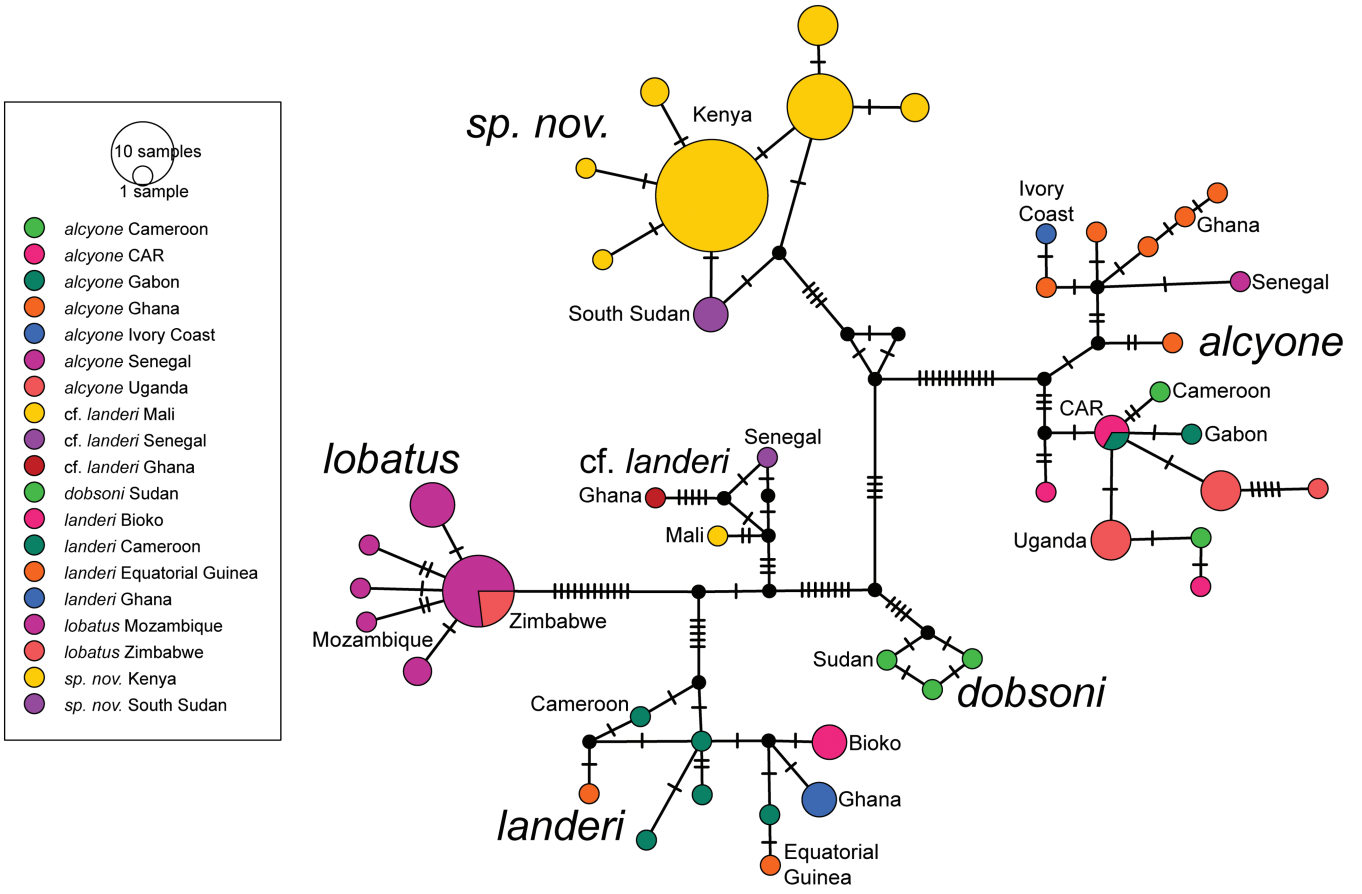

Fig. 3. Haplotype substitution network for *Cytb* among members of the *Rhinolophus landeri* species group. All but 3 haplotypes (2 for *R. alcyone*, 1 for *R. lobatus*) are restricted to a single country. "CAR" denotes haplotypes originating in the Central African Republic.

among taxa are small and overlap is high. These impressions are borne out by a principal components ordination of craniodental variables of the *landeri* complex (Supplementary Data SD2). The first 2 components account for 45.2% of overall variation. All variables had positive loadings on PC1, generally with high coefficients for skull length measures and small coefficients for dental measures. On PC2, dental measures generally had high positive coefficients while those describing braincase breadth had negative values. The projection of scores on components 1 and 2 shows broad overlap among members of the *landeri* complex.

Discriminant function analysis of the *landeri* complex offers greater separation of taxa (Supplementary Data SD3). Variables GLS, ZB, C–C, MLTLR, M2–M2, and MANDL entered the discriminant function with significance ($P < 0.05$); all but M2–M2 differed significantly among taxa in univariate analyses (Table 3). Significant Mahalanobis distances separated all taxon pairs save *dobsoni* and *lobatus* (Supplementary Data SD3). However, across taxa, only 87% of specimens were correctly classified (Supplementary Data SD4). Of 51 specimens of the clade from Kenya and South Sudan analyzed, 2 were classified as *dobsoni* and 3 as *landeri*; none were mistaken for *lobatus*. Specimens of other taxa mistaken for that clade included 1 of 2 *dobsoni*, 4 of 29 *landeri*, and 1 of 5 *lobatus*.

Echolocation calls.

Vocalization statistics for 3 of the 4 *landeri* complex taxa are tabulated in Table 4 (calls are lacking for *R. dobsoni*). Sampled taxa differ significantly in 5 of the 6 variables. All possible pairs of taxa show significant differences based on Tukey's HSD for peak frequency and end frequency (Supplementary Data SD5), with *landeri* characterized by the lowest peak frequencies (mean 102.5 kHz), and the clade from Kenya showing the highest (109.7 kHz). A scatter plot of peak frequency, end frequency, and bandwidth (Fig. 5) shows complete separation of the 3 sampled taxa.

The calls of *R. landeri* and the clade from Kenya differ qualitatively as well. Hanning call composites of 4 individual *landeri* and 4 individuals of the Kenyan clade appear in Supplementary Data SD6. The plots show that the high duty-cycle calls of these *Rhinolophus* consist of a distinct frequency-modulated element at each end of the constant-frequency band comprising most of the duration of the call and much of its energy. In *R. landeri*, the brief frequency-modulated elements are narrow-band, whereas in the clade from Kenya they are broader-banded, especially the terminal element. Also apparent in the calls of Kenyan bats is the strength of the first harmonic, which is normally obsolete in high duty-cycle bats; this harmonic is weakly expressed in only 1 of the 4 *R. landeri* but conspicuous in all 4 individuals of the Kenyan *Rhinolophus*.

Discussion

Despite morphological similarities to named forms, the strongly supported genetic distinctions of bats from Kenya and South Sudan and their qualitatively and quantitatively differentiated vocalizations clearly indicate that the Kenyan clade is a distinct lineage, which we describe as follows:

Rhinolophus webalai Patterson, Dick, Bartonjo, and Demos, new species

Webala's Horseshoe Bat

Synonymy

Rhinolophus lobatus

Matschie 1895 (in part); Hollister 1918; Swynnerton and Hayman 1950 (in part); Kulzer 1959 (in part)

Rhinolophus landeri

Ellerman et al. 1953 (in part); Kock 1969 (in part); Kingdon 1974; O'Shea and Vaughan 1980; Hill & Smith 1984 (in part); Webala et al. 2004; Taylor et al. 2005; Patterson and Webala 2012; Lanza et al. 2015; López-Baucells et al. 2017; Musila et al. 2019; Kamau et al. 2022

Rhinolophus landeri lobatus

Harrison 1961; Koopman 1975 (in part); Aggundey and Schlitter 1984; Simmons 2005 (in part); Happold 2013b (in part)

Rhinolophus cf. landeri

Demos et al. 2019; Dick et al. 2023; Rainho et al. 2023

Holotype

Field Museum of Natural History (FMNH) 215894, adult male, cleaned skull and formalin-fixed carcass in 70% ethanol, muscle tissue preserved in liquid nitrogen, and ectoparasites (6 female and 5 male streblid bat flies, all *Raymondia planiceps* Jobling, 1930) in 95% ethanol; *Cytb* sequence GenBank accession PP782749. Collected with a hand net by B.D. Patterson, P.W. Webala, and C.W. Dick (original number BDP4600) at 1830 h on 10 May 2006 from the inside walls of an abandoned building.

Type locality

Kenya: Kilifi County; Malindi Marine Park, KWS Headquarters, 5 m a.s.l., –3.2546, 40.1320, in human-modified coastal rainforest.

Etymology

We are pleased to name the new species after one of Africa's foremost bat biologists, Dr. Paul Waswa Webala, in recognition of his important contributions as a field biologist, conservation scientist, prolific author, and mentor to Africa's next generation. We suggest Webala's horseshoe bat as a common name for this species.

Diagnosis

A small member of the *R. landeri* species complex with spade-shaped sella, acutely triangular connecting process, lancet with

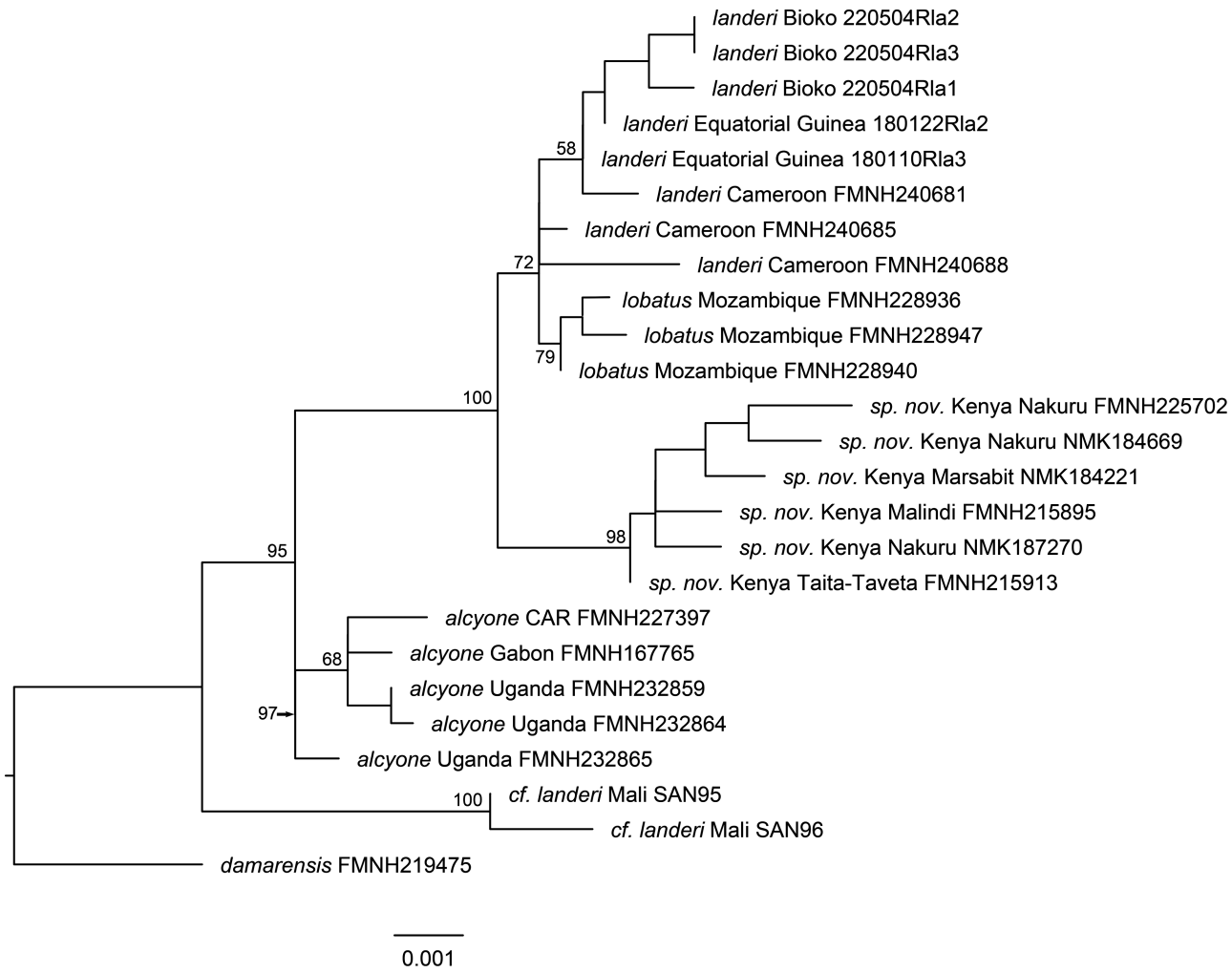

Fig. 4. Maximum likelihood analysis of 7 nuclear introns for members of the *Rhinolophus landeri* species group. The phylogeny was inferred in IQ-TREE. Bootstrap values are included at major nodes.

Table 2. External variables for species of the *landeri* species group. Entries include means, sample size (in parentheses), standard deviation, and range (minimum–maximum). Units are in mm except weight, which is in grams. Right-most column contains 1-way ANOVA results testing that the 4 groups in the *landeri* species complex (*dobsoni*, *landeri*, *lobatus*, and the new species) do not differ. n.s. denotes $P > 0.05$.

	R. alcyone	*R. dobsoni*	*R. landeri*	*R. lobatus*	R. sp. nov.	$F_{3,142}$, probability
Total length (TTL)	95.46 (13) 6.49 85 to 108	71 (1)	76.37 (19) 4.10 69 to 85	81.2 (5) 2.49 79 to 85	79.32 (128) 6.14 60 to 93	2.26 (n.s.)
Tail length (TL)	27 (13) 4.34 19 to 32	25 (1)	25.53 (19) 3.20 21 to 35	25.8 (5) 2.86 21 to 28	28.08 (128) 2.32 21 to 34	7.36 ($P < 0.001$)
Hind foot length (HF)	12.92 (13) 1.61 11 to 15	10 (1)	9.58 (19) 0.69 8 to 11	6 (5) 0.55 6 to 7	8.93 (128) 1.02 7 to 12	12.77 ($P < 0.001$)
Ear length (EL)	23.35 (13) 2.32 20 to 27	17 (1)	17.26 (19) 2.28 12 to 22	19 (5) 1.41 17 to 20	17.24 (127) 1.68 14 to 29	1.62 (n.s.)
Weight (W)	17.73 (13) 2.37 12.5 to 21	[missing]	7.45 (33) 1.28 5.2 to 9.9	8.18 (5) 0.33 7.8 to 8.6	7.80 (107) 0.68 6 to 10.2	2.88 (n.s.)
Forearm length (FA)	54.62 (13) 1.98 51 to 57	44 (1)	44.05 (40) 1.58 40 to 48	45.4 (5) 0.55 45 to 46	45.03 (128) 1.14 42.7 to 49	6.77 ($P < 0.001$)

Table 3. Craniodental variables for the *Rhinolophus landeri* species group. Entries include means, sample size (in parentheses), standard deviation, and range (minimum–maximum). Units are in mm. Right-most column contains 1-way ANOVA results testing that species of the *landeri* species complex (*dobsoni*, *landeri*, *lobatus*, and the new species) do not differ. n.s. indicates $P > 0.05$.

	R. alcyone	*R. dobsoni*	*R. landeri*	*R. lobatus*	R. sp. nov.	$F_{3,87\ to\ 112}$, probability
GLS	22.93 (13) 0.55 22.12 to 23.7	18.62 (2) 0.13 18.52 to 18.71	18.75 (34) 0.51 17.40 to 19.90	19.07 (6) 0.39 18.60 to 19.61	18.53 (61) 0.48 16.59 to 19.50	$F = 3.25$, $P = 0.025$
CIL	21.12 (9) 0.61 20.12 to 21.92	15.92 (2) 0.80 15.38 to 16.51	16.52 (30) 0.57 15.20 to 17.30	16.88 (5) 0.33 16.44 to 17.24	16.65 (54) 0.39 15.32 to 17.26	$F = 2.52$, n.s.
CCL	20.51 (13) 0.81 19.7 to 22.79	15.46 (2) 0.78 14.85 to 15.95	15.87 (35) 0.49 14.70 to 16.87	16.36 (6) 0.10 16.20 to 16.48	16.03 (60) 0.27 15.21 to 16.58	$F = 5.51$, $P = 0.001$
BB	9.67 (14) 0.28 9.24 to 10.07	8.3 (3) 0.46 7.77 to 8.65	7.91 (40) 0.27 7.10 to 8.30	8.19 (7) 0.26 7.92 to 8.62	7.98 (61) 0.32 7.39 to 8.65	$F = 2.93$, $P < 0.05$
ZB	12.14 (14) 0.36 11.56 to 12.71	9.34 (3) 0.05 9.3 to 9.4	9.29 (40) 0.35 8.40 to 9.79	9.61 (7) 0.14 9.53 to 9.90	9.59 (63) 0.23 8.93 to 10.05	$F = 10.9$, $P < 0.000$
PB	3.2 (14) 0.21 2.91 to 3.59	2.25 (3) 0.15 2.09 to 2.39	2.45 (40) 0.20 2.10 to 3.08	2.51 (7) 0.19 2.22 to 2.84	2.45 (65) 0.16 2.13 to 2.98	$F = 1.52$, n.s.
C–C	6.41 (13) 0.19 6.05 to 6.76	4.58 (3) 0.17 4.45 to 4.77	4.43 (37) 0.30 3.79 to 5.03	4.58 (7) 0.26 4.23 to 4.92	4.83 (64) 0.22 4.00 to 5.35	$F = 20.45$, $P < 0.000$
MSTW	10.47 (14) 0.22 9.87 to 10.81	8.53 (3) 0.28 8.22 to 8.77	8.46 (40) 0.29 7.70 to 9	8.68 (7) 0.11 8.55 to 8.85	8.46 (64) 0.32 7.23 to 9.25	F=1.13, n.s.
MPW	10.89 (14) 0.23 10.52 to 11.21	8.93 (2) 0.12 8.84 to 9.01	8.95 (38) 0.25 8.50 to 9.60	9.03 (7) 0.17 8.86 to 9.34	8.65 (60) 0.60 8.72 to 9.6	$F = 3.86$, $P = 0.1$.
MTRL	8.79 (13) 0.24 8.42 to 9.17	6.44 (3) 0.21 6.23 to 6.64	6.58 (38) 0.31 5.80 to 7.08	6.74 (7) 0.15 6.43 to 6.92	6.64 (66) 0.20 5.922 to 7.00	$F = 1.61$, n.s
MLTRL	6.79 (14) 0.21 6.52 to 7.13	5.26 (3) 0.04 5.22 to 5.29	5.03 (40) 0.24 4.60 to 5.63	5.35 (7) 0.13 5.22 to 5.54	5.06 (66) 0.21 4.76 to 5.64	$F = 5.40$, $P < 0.002$
M2–M2	8.55 (14) 0.27 8.06 to 8.99	6.44 (3) 0.14 6.29 to 6.55	6.61 (40) 0.20 6.30 to 7.10	6.57 (7) 0.20 6.26 to 6.80	6.62 (66) 0.27 6.1 to 7.21	$F = 0.62$, n.s.
DENL	15.96 (14) 0.55 15.19 to 16.8	11.78 (2) 0.63 11.33 to 12.22	12.03 (40) 0.46 11.20 to 13.30	12.43 (7) 0.10 12.28 to 12.57	12.17 (65) 0.35 11.47 to 12.82	$F = 3.15$, $P < 0.05$
MANDL	7.13 (66) 0.19 6.76 to 7.58	6.93 (2) 0.21 6.79 to 7.08	7.42 (39) 0.39 6.3 to 8.3	7.35 (7) 0.22 7.01 to 7.66	7.13 (66) 0.19 6.75 to 7.58	$F = 10.4$, $P < 0.000$

strongly concave tip, and the presence of rust-colored axillary tufts in a majority of adult males (Fig. 6). Middle lower premolar tiny, displaced labially and barely reaching the cingula of flanking premolars (Fig. 7). Echolocation call (Supplementary Data SD6) dominated by long constant-frequency signal flanked by brief initial and terminal frequency-modulated elements, the latter with a greater frequency span, making call bandwidth very broad. Peak frequency averages 109.7 kHz, end frequency 80.2 kHz, and bandwidth 30.2 kHz. Unlike other sampled members of the *landeri* complex, the fundamental (first) harmonic of the call is conspicuous.

Description and comparisons

External measurements (in mm unless otherwise noted) of the holotype are TTL 76, TL 26, HF10, EL 15, WT 9.8 g, FA 44.5; tibia length, 19.18; third metacarpal, 31.45. Craniodental measurements are GLS 18.5, CIL 16.6, CCL 15.99, BB 7.69, ZB 9.47, PB 2.48, C–C 4.91,

Table 4. Call variables for 3 species of the *Rhinolophus landeri* complex. Entries include means, sample size (in parentheses), standard deviation, and range (minimum–maximum). Units are in kHz unless otherwise noted. Right-most column contains 1-way ANOVA results testing that the 3 groups do not differ.

	R. landeri	*R. lobatus*	R. sp. nov.	$F_{2,40}$, probability
Frequency of maximum energy	102.45 (14) 1.00 100.91 to 103.87	106.88 (5) 0.55 106.58 to 107.87	109.73 (24) 1.17 105.53 to 110.70	203.54 ($P < 0.001$)
Start frequency	104.83 (14) 1.94 102.56 to 111.71	111.56 (5) 0.53 111.32 to 112.50	110.41 (24) 1.26 105.93 to 111.71	73.95 ($P < 0.001$)
End frequency	87.07 (14) 6.38 81.32 to 100.50	103.47 (5) 0.52 103.12 to 104.29	80.23 (24) 3.62 75.47 to 89.53	55.57 ($P < 0.001$)
Duration (ms)	67.56 (14) 14.76 32.61 to 85.07	65.70 (5) 15.52 47.95 to 85.05	58.87 (24) 9.37 47.60 to 85.00	2.50 (n.s.)
Call interval (ms)	124.73 (5) 83.26 76.00 to 272.53	138.36 (5) 45.93 87.85 to 198.55	177.55 (24) 36.45 113.30 to 293.30	3.58 ($P < 0.05$)
Bandwidth	12.29 (14) 6.61 3.45 to 23.22	8.08 (5) 0.26 7.62 to 8.21	30.17 (24) 3.92 19.31 to 35.58	143.55 ($P < 0.001$)

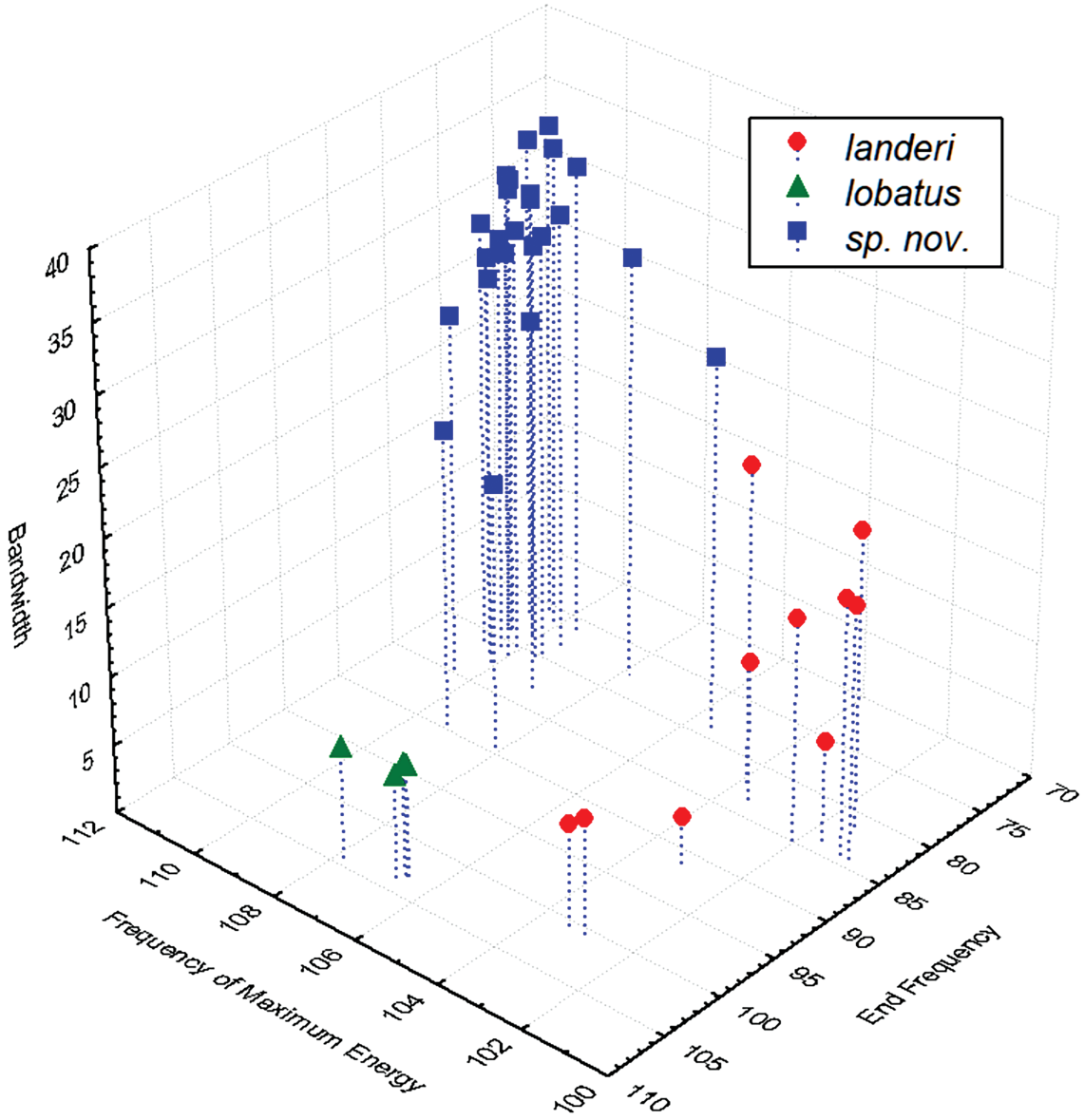

Fig. 5. Trivariate plot of echolocation call variables for sampled members of the *Rhinolophus landeri* species complex. Variables are frequency of maximum energy, end frequency, and bandwidth; units of all 3 in kHz.

Fig. 6. External characteristics of *Rhinolophus webalai* sp. nov., showing nose leaf, axillary tufts, and typical grayish-brown pelage condition of FMNH 233830, adult male from Marsabit National Park and Reserve, Kenya.

MSTW 7.73, MPW 8.57, MTRL 6.62, MLTRL 4.91, M2–M2 6.32, DENL 11.91, MANDL 7.18.

A small member of the *R. landeri* species complex with naked, spade-shaped sella; acutely triangular connecting process, with leading and trailing edges longer than its base on the lancet; tip of the lancet acutely triangular, with lancet margins strongly constricted above the dorsal cell; lancet shorter than the horseshoe is broad; horseshoe less broad than muzzle, and averaging somewhat smaller than in *R. landeri* and *R. lobatus*—mean of 6 fluid-preserved samples 7.1 mm with a range 6.76 to 7.74, whereas comparable values for 12 *landeri* are 7.53 mm (6.9 to 8.3) and 6 *lobatus* are 7.61 mm (7.07 to 7.98), but differences are not significant ($F_{2,21}$ = 2.96, P = 0.07). Median emargination of horseshoe as broad as the connecting process, and internarial cup is highly cupped. Lower lip with a single distinct median groove. Dorsal fur typically grayish to honey brown, venter paler. Many rhinolophoid bats, including both *R. alcyone* and *R. landeri* (Rosevear 1965), exhibit 2 pelage morphs—one grayish-brown and the other distinctly reddish. Although the reddish morph was thought to be absent in *R. dobsoni* (cf. Kock 1969), FMNH 35381 from Gallabat, Sudan (near the Ethiopian border), documents its existence in that taxon. The reddish morph is also rare and may be entirely absent in *R. webalai* sp. nov., as none of the specimens we collected in mistnets, abandoned buildings, mines, or caves exhibited this morph. Rust-colored axillary tufts are present in most males. Of 33 fluid-preserved males at hand, 18 had well developed rust-colored axillary tufts, and 5 others had incipient (or rudimentary) tufts; only 10 lacked any trace of tufts.

First upper premolar small but aligned with adjacent teeth so that canine and second premolar (P^3) are well separated (Supplementary Data SD7); middle lower premolar tiny, its crown barely reaching the cingula of the adjacent premolars, and labially displaced, so that the first and last premolars are in contact or very nearly so. *Rhinolophus dobsoni* resembles it in lower premolar size and placement, whereas *R. landeri* and *R. lobatus* have somewhat larger and less displaced p3.

Although traditional cranial and dental morphometrics of species in the *landeri* complex are broadly overlapping, a number of variables show significant diagnostic differences ($P < 0.05$) as judged by Tukey's HSD. From *R. dobsoni*, *R. webalai* sp. nov. differs in having a narrower braincase and a shorter postcanine maxillary toothrow. From *R. landeri*, the new species differs in having broader zygomatic arches, a greater distance across the canines, a smaller mastoid process width, and shorter mandibular toothrow. And from *R. lobatus*, *R. webalai* sp. nov. differs in having a shorter postcanine maxillary toothrow (Table 3; Fig. 7).

The baculum of *R. webalai* sp. nov. is a simple, straight rod-like shaft with a smoothly flaring and slightly notched base when viewed dorsally. Across 9 adult males, bacular length averaged 2.25 mm (range 2.05 to 2.49) and base breadth 0.78 mm (0.685 to 0.885; Supplementary Data SD8). Bats identified as *R. lobatus* by Taylor et al. (2018) had on average somewhat longer and broader bacula (2.57 mm, 0.94 mm), although several small samples of bats that they identified as *R.* cf. *lobatus* from the same general area varied in average baculum length from 1.98 to 2.96 mm and in base breadth from 0.42 to 1.12 mm. A single West African bat that they identified as *R. landeri* had a baculum with a length of 2.29 mm and a breadth of 0.88 mm, resembling *R. webalai* sp. nov.

Echolocation calls of *R. webalai* sp. nov. (Fig. 5; Supplementary Data SD6) are dominated by a long constant-frequency signal (mean 109.76 kHz); call frequency averages higher than either *R. landeri* (102.7 kHz) or *R. lobatus* (106.9 kHz). The main call in all 3 species is flanked initially and terminally by brief frequency-modulated elements; the terminal element in *R. webalai* sp. nov. has a great frequency span, making the bandwidth very broad (30.17 kHz) for a high duty-cycle bat, and much broader than *R. landeri* (9.03 kHz) or *R. lobatus* (8.08 kHz). The fundamental (first) harmonic is conspicuous in *R. webalai* sp. nov. but not apparent in calls of *R. landeri* or *R. lobatus*.

Known parasites of *R. webalai* sp. nov. include the streblid bat fly *Raymondia planiceps*, which infested the series from Malindi Marine Park and Marsabit National Park. Bats of this species are also more rarely infested by the eurytopic nycteribiid bat fly *Penicillidia fulvida* (Bigot 1885; see Verrett et al. 2022).

Distribution

Insofar as known, *R. webalai* sp. nov. occurs in a variety of habitats, both natural and human-influenced, in Kenya and South Sudan. Its occurrence in neighboring Uganda and northern Tanzania seems

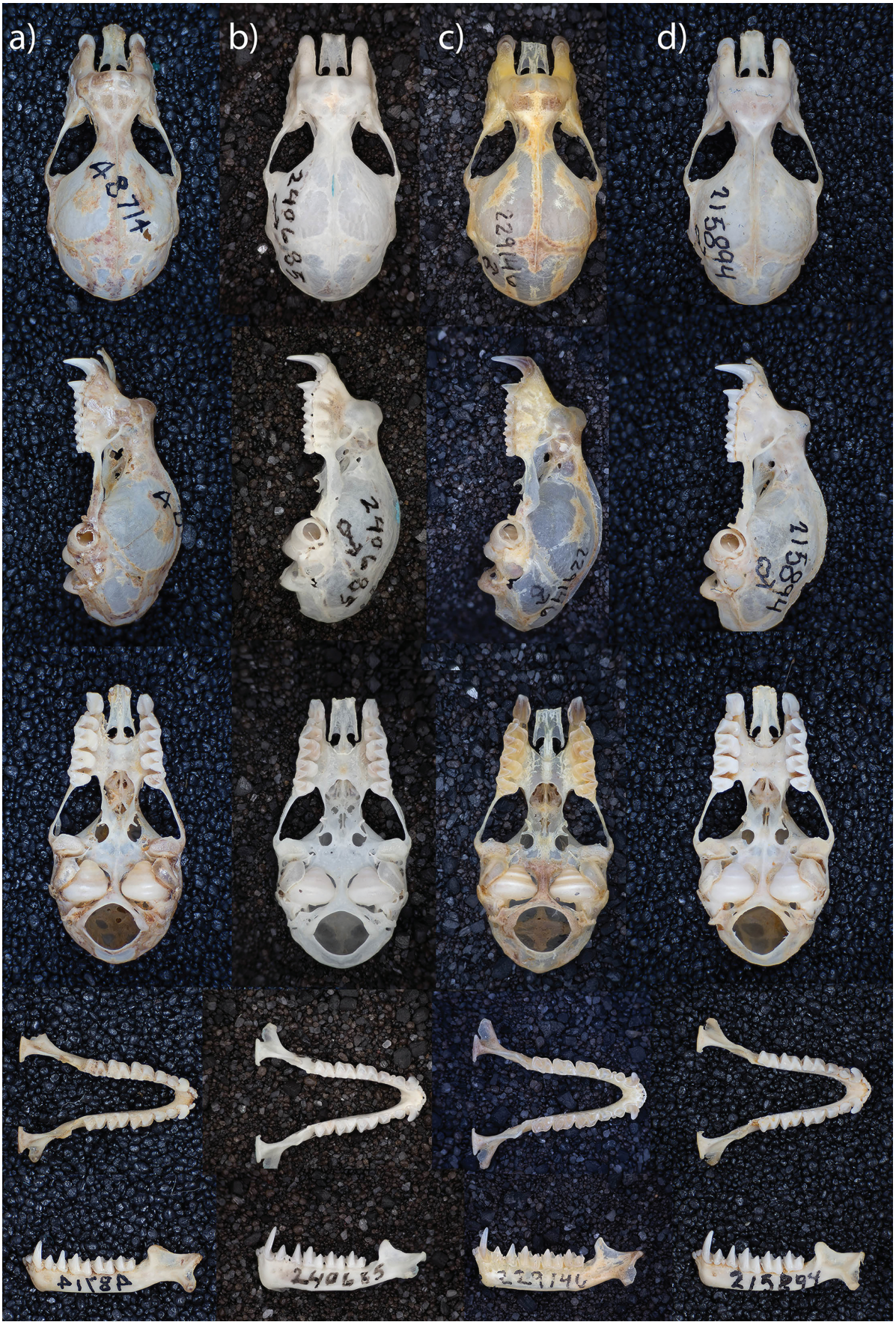

Fig. 7. Cranial and mandibular views of the *Rhinolophus landeri* species complex, all to same scale: (a) *R. dobsoni*, FMNH 48714; (b) *R. landeri*, FMNH 240685; (c) *R. lobatus*, FMNH 229146; and (d) *R. webalai* sp. nov., FMNH 215894 (holotype).

likely. Somali bats identified as *R. landeri* by Lanza et al. (2015) have measurements distinctly smaller than those of *R. webalai*, raising the possibility that the new species is replaced by a different species in northern parts of that country. The extensive distribution and varied ecological and roosting associations of *R. webalai* suggest an IUCN listing as "Least Concern."

For most of the 20th century, the *R. landeri* complex was thought to consist of a single species, more recently as one consisting of 2 subspecies. As might be expected from this history, traditional external and craniodental characters fail to distinguish the different members of this group. Yet as alternative character sets are documented, the distinctions of regional taxa have become more apparent. Mitochondrial *Cytb* shows reciprocal monophyly among all the taxa tested, including *R. dobsoni*, while 7 nuclear introns more clearly document the distinction of *R. webalai* sp. nov. from other members of this complex than is apparent between *R. landeri* and *R. lobatus*. Small but significant differences also exist in the vocalizations of typical members of *R. landeri*, *R. lobatus*, and *R. webalai* sp. nov., and the calls of the latter species appear to differ qualitatively in call structure.

Strong genetic and vocal distinctions of *R. webalai* sp. nov. are the primary justifications for its description as a new species, yet these character sets are still lacking for some other taxa in the complex. Only mitochondrial sequences are available to gauge the genetic distinctions of *R. webalai* sp. nov. from Sudanese *R. dobsoni*. The *Cytb* phylogeny securely recovered *R. webalai* and *R. dobsoni* as monophyletic and as sister to each other and as a pair to *R. landeri* (Fig. 2). The substitution network also substantiates the distinction of *R. dobsoni* from both *R. landeri* and from *R. webalai* sp. nov. (Fig. 3).

Rhinolophus axillaris, known only from Aba, Democratic Republic of the Congo, has long been treated as a synonym of *R. landeri* (Koopman 1975; Van Cakenberghe et al. 2017), and thus was a possible senior synonym for the new species. *Rhinolophus axillaris* was named in recognition of its possession of the axillary tufts that characterize other members of the *landeri* species group. However, in GLS (mean of 20 mm reported by Allen et al. 1917), *axillaris* is larger than any individual of the *landeri* complex that we measured, and those species average far smaller (Table 3). Perhaps more significantly, the second premolar in the mandibular battery of *axillaris* is large and more in line with the remaining cheek teeth, fully separating the first lower premolar from the last (Supplementary Data SD9). In all members of the *landeri* complex, the second lower premolar is tiny, subequal to the cingula on flanking premolars and labially displaced, so that the first and last premolars are in closer contact (Fig. 7; Supplementary Data SD7). Unfortunately, our efforts to obtain *Cytb* sequence from the *R. axillaris* holotype failed. Until additional specimens allow a fuller evaluation and characterization of this form, we regard *R. axillaris* as a valid taxon. Given its axillary tufts, it is most likely a member of the *landeri* species group; perhaps given its size, it is more closely related to *R. alcyone* or *R. guineensis* than to the *landeri* complex.

Our *Cytb* substitution network (Fig. 3) neatly recovers members of the *landeri* species group as nearest neighbors and admits no other species. A previous median-joining network for these taxa (Fig. 3 in Taylor et al. 2018) depicted various species of the *Rhinolophus capensis* species group interposed between *R. lobatus* and *R. landeri*. This undoubtedly resulted from use of a contaminated sample for *R. landeri*, as acknowledged by Taylor et al. (2019). Interestingly, in mitochondrial terms, *lobatus* is closer to West African "cf. *landeri*" than it is to its erstwhile synonyms and geographic neighbors: Central African *landeri*, North African *dobsoni*, and East African *webalai* sp. nov. (Table 1).

Both *R. alcyone* and *R. landeri* show evidence of distinct subclades in Central and West Africa (Figs. 2 and 3). The phylogeographic break in *R. alcyone* occurs at the Dahomey Gap, where the interior savanna mosaic extends south to the coast and interrupts the expanse of moist equatorial rainforests (Demenou et al. 2016). The gap itself is demarcated by the 2 largest rivers in West Africa, the Volta and the Niger, adding additional barriers to biotic distributions (Oates et al. 2022). Samples of *R. alcyone* collected immediately west of the gap in Ghana were all recovered in a clade with those from Ivory Coast and Senegal, well separated from the Central African clade. This species is closely associated with lowland rainforests (Happold 2013a). In *R. landeri*, both the West African subclade (labeled as cf. *landeri* in Fig. 1) and the Central African clade range into Ghana, so that the distribution of the latter clade spans the Dahomey Gap. The broad habitat tolerances of *R. landeri*, which can include degraded forests and woodlands in West Africa (Rosevear 1965), and the dispersal abilities that allowed it to reach Bioko Island in the Gulf of Guinea may have allowed the Central African clade to cross the gap.

Cytb sequences from Mali (KU531353) and Senegal (FJ457612) were accessioned in GenBank as *R. landeri* and taken to represent that species in the corrected analysis by Taylor et al. (2019). These West African sequences, here designated cf. *landeri*, were strongly supported as sister to, but well separated from, the typical Central African *landeri* clade in the mitochondrial analysis (Fig. 2); in the multi-locus intron analysis, they were recovered as sister to all remaining members of the *landeri* species group (Fig. 4). The only species of the *landeri* species group not explicitly included in our analysis was *R. guineensis*, whose geographic range includes Guinea, Senegal, and likely also Mali. Mitochondrial–nuclear discordance is well known in *Rhinolophus* bats (e.g., Mao et al. 2013; Demos et al. 2019) and is apparent here. Until vouchered specimens of *R. guineensis* can be sequenced, it is possible that the specimens labeled cf. *landeri* in Fig. 4 are in fact misidentified *R. guineensis*; their association with the West African *Cytb* clade of *R. landeri* is perhaps attributable to a historic introgression event.

Vocalizations distinguish *R. webalai* sp. nov. from other members of the *landeri* species complex, particularly its very low terminal frequencies and the strength of the first harmonic in its calls. Both features had been noted in earlier studies of Kenyan "*R. landeri*." Using early acoustic equipment, O'Shea and Vaughan (1980) reported the peak frequency of handheld *R. webalai* sp. nov. calls as 55 kHz, mistaking its fundamental frequency for the second harmonic—in most rhinolophoid bats, the fundamental component is suppressed, and only the second harmonic is apparent. Taylor et al. (2005) later recognized the 55 kHz band as the fundamental frequency of the Kenyan bats.

Although the calls of most high duty-cycle bats are dominated by a constant frequency, Hill and Smith (1984) noted that "some populations" of *R. landeri* have calls with frequency-modulated sweeps of up to 40 kHz. This is an apparent reference to the vocalizations of *R. webalai* sp. nov., as frequency-modulated sweeps in the calls of both *R. landeri* and *R. lobatus* have very modest bandwidths by comparison (Fig. 5; Supplementary Data SD6).

Our conclusions (1) that the *R. landeri* complex includes not 2 but 4 species (*R. landeri*, *R. lobatus*, *R. dobsoni*, and *R. webalai* sp. nov.) and (2) that *R. axillaris* is distinct and possibly more distantly related to this group must be considered tentative: our sample sizes were small and our geographic sampling porous. Basing our analysis on samples collected near type localities with supporting genetic information strengthens the association between pattern and name, aiding taxonomic characterization, but ignores geographic variation and fails to interrogate zones of contact. Our conclusions rest mainly on the integrity of the genetic and

vocalization characters we have presented. Another potentially informative character set for subsequent analyses would be more detailed study of nose leaf variation (Csorba et al. 2003). Unfortunately, the methodology and analysis recently described by Chornelia et al. (2022) for distinguishing Asian species of *Rhinolophus* cannot be retroactively conducted on the dried or fluid-preserved museum specimens on which we based our analysis. Nevertheless, future field workers should evaluate its effectiveness for these Afrotropical *Rhinolophus*.

Supplementary data

Supplementary data are available at *Journal of Mammalogy* online.

Supplementary Data SD1. Table of specimens used in genetic, morphological, and vocalization analyses of the *Rhinolophus landeri* species group, including accession numbers and provenance (.csv format).

Supplementary Data SD2. Plot of PCA factors 1 and 2 from analysis of craniodental variables for the *Rhinolophus landeri* complex.

Supplementary Data SD3. Squared Mahalanobis distances from discriminant function analysis of log-transformed craniodental variables, and their *F*-values and significance.

Supplementary Data SD4. Classification matrix from discriminant function analysis and percent correctly classified values.

Supplementary Data SD5. Results of Tukey's HSD (unequal sample sizes) for 6 vocalization variables among sampled members of the *Rhinolophus landeri* complex.

Supplementary Data SD6. Hanning window plots of 4 individuals of *Rhinolophus landeri* field recorded in Equatorial Guinea (a to d), and 4 individuals of *Rhinolophus webalai* sp. nov. from Kenya (e to h). Ordinal units in kHz; abscissa panels are each 250 ms.

Supplementary Data SD7. Maxillary (above) and mandibular (below) toothrows of *Rhinolophus webalai* sp. nov. (FMNH 215909). Scale bar = 1 mm.

Supplementary Data S8. Dorsal view of bacula of *Rhinolophus webalai* sp. nov.; scale below in mm. (a) FMNH 233843; (b) FMNH 233883; (c) FMNH 233884; (d) FMNH 233885; (e) FMNH 233894.

Supplementary Data S9. Mandibular toothrow of *Rhinolophus axillaris* (AMNH 49175, female holotype) showing the prominent second lower premolar that clearly separates the first and last premolars, suggesting it may not belong in the *Rhinolophus landeri* complex.

Acknowledgments

We are grateful to Simon Musila and the National Museums of Kenya for help with loans of the new species. We thank curators and staff at the American Museum of Natural History (New York), Royal Ontario Museum (Toronto), Natural History Museum (London), and the Museum für Naturkunde (Berlin) for access to key specimens and permission to sample and measure them. Steve Goodman kindly allowed us access to samples that he collected of *R. lobatus*. Tharaka Kusuminda kindly supplied us with photos of the type series of *R. lobatus* and Luisa Gasparetto with photos of the holotype of *R. axillaris*. We are most grateful to Stephanie Ware, of the Collaborative Invertebrate Laboratories at FMNH, for her expertise in generating the images included in Fig. 7 and Supplementary Data SD7. The authors thank their collaborators, field assistants, and funding agencies during the fieldwork that originally led to vouchers and data collected from Kenya, Mozambique, Uganda, South Sudan, Cameroon, Equatorial Guinea, and Ghana. They also thank their home institutions as well as all individuals who contributed to our taxonomic infrastructure through contributions either to public museums or to genome repositories.

Author contributions

BDP, TCD, and JJ conceived the study. BDP and LT collected skull measurements from museum specimens. TCD, MMM, ALG, CM, LT, and JJ acquired DNA sequences. LT, ALG, CM, MCS, and Paul Webala recorded and analyzed vocalizations. BDP performed the morphometric and vocal analyses, TCD performed genetic analyses, and both wrote the first draft. All authors contributed to funding acquisition, fieldwork, specimen collection, data acquisition, and edited and approved the final version of the manuscript.

Funding

None declared.

Conflict of interest

None declared.

Data availability

GenBank accession numbers for all sequences used appear in Supplementary Data SD1; the alignments used are archived on Mendeley Data (DOI: 10.17632/mxgyjsj66t.1).

References

Aggundey IR, Schlitter DA. 1984. Annotated checklist of the mammals of Kenya. I. Chiroptera. Annals of the Carnegie Museum 53(5):119–161. https://doi.org/10.5962/p.330478

Allen JA, Lang H, Chapin JP. 1917. The American Museum Congo Expedition collection of bats. Bulletin of the American Museum of Natural History 37(18):405–563.

Andersen K. 1906. On some new or little-known bats of the genus *Rhinolophus* in the collection of the Museo Civico, Genoa. Annali del Museo Civico di Storia Naturali di Genova, Serie 3a 2(42):173–195.

Beja P, Vaz Pinto P, Veríssimo L, Bersacola E, Fabiano E, Palmeirim JM, Monadjem A, Monterroso P, Svensson MS, Taylor PJ. 2019. The mammals of Angola. In: Huntley BJ, Russo V, Lages F, Ferrand N, editors. Biodiversity of Angola: science & conservation: a modern synthesis. Cham (Switzerland): Springer; p. 357–443. http://doi.org/10.1007/978-3-030-03083-4_15

Bickham JW, Patton JC, Schlitter DA, Rautenbach IL, Honeycutt RL. 2004. Molecular phylogenetics, karyotypic diversity, and partition of the genus *Myotis* (Chiroptera: Vespertilionidae). Molecular Phylogenetics and Evolution 33(2):333–338. https://doi.org/10.1016/j.ympev.2004.06.012

Bickham JW, Wood CC, Patton JC. 1995. Biogeographic implications of cytochrome b sequences and allozymes in sockeye (*Oncorhynchus nerka*). The Journal of Heredity 86(2):140–144. https://doi.org/10.1093/oxfordjournals.jhered.a111544

Bücs S-L, Csorba G. 2022. Blasius's horseshoe bat *Rhinolophus blasii* Peters, 1867. In: Hackländer K, Zachos FE, editors. Handbook of the mammals of Europe. Switzerland: Springer; p. 1–24. https://doi.org/10.1007/978-3-319-65038-8_41-1

Chornelia A, Hughes AC. 2022. The evolutionary history and ancestral biogeographic range estimation of Old-World Rhinolophidae and Hipposideridae (Chiroptera). BMC Ecology and Evolution 22(1):112. https://doi.org/10.1186/s12862-022-02066-x

Chornelia A, Lu J, Hughes AC. 2022. How to accurately delineate morphologically conserved taxa and diagnose its phenotypic disparities: a species delimitation in cryptic Rhinolophidae (Chiroptera)

of Asia lineages. Frontiers in Ecology and Evolution 10:854509. http://doi.org/10.3389/fevo.2022.854509

Csorba G. 2008. Taxonomy of the horseshoe bats of the world (Chiroptera: Rhinolophidae) [PhD thesis]. Debrecen (Hungary): Debrecen University; 172 pp.

Csorba G, Ujhelyi P, Thomas N. 2003. Horseshoe bats of the world (Chiroptera: Rhinolophidae). Shrewsbury (England): Alana Books; xxxii + 160 pp.

Demenou BB, Piñeiro R, Hardy OJ. 2016. Origin and history of the Dahomey Gap separating West and Central African rain forests: insights from the phylogeography of the legume tree *Distemonanthus benthamianus*. Journal of Biogeography 43(5):1020–1031. https://doi.org/10.1111/jbi.12688

Demos TC, Webala PW, Bartonjo M, Patterson BD. 2018. Hidden diversity of African yellow house bats (Vespertilionidae, *Scotophilus*): insights from multilocus phylogenetics and lineage delimitation. Frontiers in Ecology and Evolution 6:86. https://doi.org/10.3389/fevo.2018.00086

Demos TC, Webala PW, Goodman SM, Kerbis Peterhans JC, Bartonjo M, Patterson BD. 2019. Molecular phylogenetics of the African horseshoe bats (Chiroptera: Rhinolophidae): expanded geographic and taxonomic sampling of the Afrotropics. BMC Evolutionary Biology 19(1):166. https://doi.org/10.1186/s12862-019-1485-1

Dick CW, Verrett TB, Webala PW, Patterson BD. 2023. Nycteribiid bat flies (Arthropoda, Insecta, Diptera, Nycteribiidae) of Kenya. ZooKeys 1169:65–85. https://doi.org/10.3897/zookeys.1169.102800

Dool SE, Puechmaille SJ, Foley NM, Allegrini B, Bastian A, Mutumi GL, Maluleke TG, Odendaal LJ, Teeling EC, Jacobs DS. 2016. Nuclear introns outperform mitochondrial DNA in inter-specific phylogenetic reconstruction: lessons from horseshoe bats (Rhinolophidae: Chiroptera). Molecular Phylogenetics and Evolution 97(4):196–212. https://doi.org/10.1016/j.ympev.2016.01.003

Eisentraut M. 1960. Zwei neue Rhinolophiden aus Guinea. Stuttgarter Beiträge zur Naturkunde 39:1–7.

Ellerman J, Morrison-Scott T, Hayman E. 1953. Southern African mammals 1758 to 1951: a reclassification. London: British Museum (Natural History); 363 pp.

Fenton MB, Faure PA, Ratcliffe JM. 2012. Evolution of high duty cycle echolocation in bats. The Journal of Experimental Biology 215(Pt 17):2935–2944. https://doi.org/10.1242/jeb.073171

Guillen Servent A, Francis CM, Ricklefs RE. 2003. Phylogeny and biogeography of the horseshoe bats. In: Csorba G, Ujhelyi P, Thomas N, editors. Horseshoe bats of the world (Chiroptera: Rhinolophidae). Shropshire (England): Alana Books; p. xii–xxiv.

Happold M. 2013a. *Rhinolophus alcyone* Halcyon Horseshoe Bat. In: Happold M, Happold DCD, editors. The mammals of Africa, vol. 4: hedgehogs, shrews and bats. London: Bloomsbury Publishing; p. 311–312.

Happold M. 2013b. *Rhinolophus landeri* Lander's horseshoe bat. In: Happold M, Happold DCD, editors. The mammals of Africa, vol. 4: hedgehogs, shrews and bats. London: Bloomsbury Publishing; p. 340–341.

Harrison DL. 1961. A checklist of the bats (Chiroptera) of Kenya Colony. Journal of the East African Natural History Society 23(7):286–294.

Hill JE, Smith JD. 1984. Bats, a natural history. London: British Museum (Natural History); 233 pp.

Hiryu S, Mora EC, Riquimaroux H. 2016. Behavioral and physiological bases for Doppler shift compensation by echolocating bats. In: Fenton MB, Grinnell A, Popper A, Fay R, editors. Bat bioacoustics, Springer handbook of auditory research, vol. 54. New York (NY, USA): Springer; p. 239–263. https://doi.org/10.1007/978-1-4939-3527-7_9

Hollister N. 1918. East African mammals in the United States National Museum. Part 1. Insectivora, Chiroptera, and Carnivora. Bulletin of the United States National Museum 99:1–194 + 155 pls. https://doi.org/10.5962/bhl.part.21107

Igea J, Juste J, Castresana J. 2010. Novel intron markers to study the phylogeny of closely related mammalian species. BMC Evolutionary Biology 10(1):1–13. https://doi.org/10.1186/1471-2148-10-369

Jung K, Molinari J, Kalko EKV. 2014. Driving factors for the evolution of species-specific echolocation call design in New World free-tailed bats (Molossidae). PLoS One 9(1):e85279. https://doi.org/10.1371/journal.pone.0085279

Kamau J, Ergunay K, Webala PW, Justi SA, Bourke BP, Kamau MW, Hassell J, Chege MN, Mwaura DK, Simiyu C, *et al*. 2022. A novel coronavirus and a broad range of viruses in Kenyan cave bats. Viruses 14(12):2820. https://doi.org/10.3390/v14122820

Kingdon J. 1974. East African mammals. An atlas of evolution in Africa. 2A. Insectivores and bats. London: Academic Press; xlix + 341 pp.

Kock D. 1969. Die fledermaus-fauna des Sudan (Mammalia, Chiroptera). Abhandlungen der Senckenbergischen Gesellschaft für Naturforschung 521:1–238.

Koopman KF. 1975. Bats of the Sudan. Bulletin of the American Museum of Natural History 154(4):353–444. http://hdl.handle.net/2246/609

Koopman KF. 1989. Systematic notes on Liberian bats. American Museum Novitates 2946:1–11. http://hdl.handle.net/2246/5100

Krueger F. 2017. TrimGalore v.0.4.3, released 25 Jan 2017. https://www.bioinformatics.babraham.ac.uk/projects/trim_galore/

Kulzer E. 1959. Fledermause aus OstAfrika: uber eine sammlung von Chiropteran aus Kenia und Tanganyika mit ethologischen und okologischen Beobachtungen. Zoologische Jahrbücher Abteilung für Systematik, Okologie und Geographie der Tiere 87(1/2):13–42.

Kumar S, Stecher G, Li M, Knyaz C, Tamura K. 2018. MEGA X: molecular evolutionary genetics analysis across computing platforms. Molecular Biology and Evolution 35(6):1547–1549. https://doi.org/10.1093/molbev/msy096

Lanza B, Funaioli U, Riccucci M. 2015. The bats of Somalia and neighbouring areas. Frankfurt am Main (Germany): Edition Chimaira; 566 pp.

Leigh JW, Bryant D. 2015. POPART: full-feature software for haplotype network construction. Methods in Ecology and Evolution 6(9):1110–1116. https://doi.org/10.1111/2041-210x.12410

Li H, Durbin R. 2011. Inference of human population history from individual whole-genome sequences. Nature 475(7357):493–496. https://doi.org/10.1038/nature10231

López-Baucells A, Rocha R, Webala P, Nair A, Uusitalo R, Sironen T, Forbes KM. 2017. Rapid assessment of bat diversity in the Taita Hills Afromontane cloud forests, southeastern Kenya. Barbastella 9(1):1–12. https://doi.org/10.14709/BarbJ.9.1.2016.04

Magoč T, Salzberg SL. 2011. FLASH: fast length adjustment of short reads to improve genome assemblies. Bioinformatics 27(21):2957–2963. https://doi.org/10.1093/bioinformatics/btr507

Mammal Diversity Database. 2023. Mammal Diversity Database (version 1.12.1) [data set]. Zenodo. https://doi.org/10.5281/zenodo.10595931

Mao X, Thong VD, Bates PJ, Jones G, Zhang S, Rossiter SJ. 2013. Multiple cases of asymmetric introgression among horseshoe bats detected by phylogenetic conflicts across loci. Biological Journal of the Linnean Society 110(2):346–361. https://doi.org/10.1111/bij.12138

Mao X, Tsagkogeorga G, Thong VD, Rossiter SJ. 2019. Resolving evolutionary relationships among six closely related taxa of the horseshoe bats (*Rhinolophus*) with targeted resequencing data. Molecular Phylogenetics and Evolution 139(10):106551. https://doi.org/10.1016/j.ympev.2019.106551

Martin W. 1838. Description of a new bat (*Rhinolophus landeri*) from Fernando Po, and a new hedgehog (*Erinaceus concolor*) from Trebizond. Proceedings of the Zoological Society of London 1837(5):101–103.

Matschie P. 1895. Die Säugethiere Deutsch-Ost-Afrikas. Berlin: Dietrich Reimer; 157 pp.

Matthee CA, Burzlaff JD, Taylor JF, Davis SK. 2001. Mining the mammalian genome for artiodactyl systematics. Systematic Biology 50(3):367–390. https://doi.org/10.1080/10635150119683

McDonough MM, Parker LD, Rotzel McInerney N, Campana MG, Maldonado JE. 2018. Performance of commonly requested destructive museum samples for mammalian genomic studies. Journal of Mammalogy 99(4):789–802. https://doi.org/10.1093/jmammal/gyy080

Minh BQ, Schmidt HA, Chernomor O, Schrempf D, Woodhams MD, von Haeseler A, Lanfear R. 2020. IQ-TREE 2: new models and efficient methods for phylogenetic inference in the genomic era. Molecular Biology and Evolution 37(5):1530–1534. https://doi.org/10.1093/molbev/msaa015

Moir HM, Jackson JC, Windmill JF. 2013. Extremely high frequency sensitivity in a 'simple' ear. Biology Letters 9(4):20130241. https://doi.org/10.1098/rsbl.2013.0241

Moreau KE, Hopkins GHE, Hayman RW. 1946. The type-localities of some African mammals. Proceedings of the Zoological Society of London 115(3–4):387–447. https://doi.org/10.1111/j.1096-3642.1946.tb00101.x

Musila S, Monadjem A, Webala PW, Patterson BD, Hutterer R, De Jong YA, Butynski TM, Mwangi G, Chen Z-Z, Jiang X-L. 2019. An annotated checklist of mammals of Kenya. Zoological Research 40(1):3–52. https://doi.org/10.24272/j.issn.2095-8137.2018.059

O'Shea TJ, Vaughan TA. 1980. Ecological observations on an East-African bat community. Mammalia 44(4):485–496. https://doi.org/10.1515/mamm.1980.44.4.485

Oates JF, Woodman N, Gaubert P, Sargis EJ, Wiafe ED, Lecompte E, Dowsett-Lemaire F, Dowsett RJ, Gonedelé Bi S, Ikemeh RA, *et al*. 2022. A new species of tree hyrax (Procaviidae: *Dendrohyrax*) from West Africa and the significance of the Niger–Volta interfluvium in mammalian biogeography. Zoological Journal of the Linnean Society 194(2):527–552. https://doi.org/10.1093/zoolinnean/zlab029

Patterson BD, Webala PW. 2012. Keys to the bats (Mammalia: Chiroptera) of East Africa. Fieldiana: Life and Earth Sciences 6(1):1–60. https://doi.org/10.3158/2158-5520-12.6.1

Peters WCH. 1852. Naturwissenschaftliche Reise nach Mossambique: auf Befehl Seiner Majestät des Königs Friedrich Wilhelm IV, in den Jahren 1842 bis 1848 ausgeführt. Zoologie. 1. Säugethiere. Berlin: Georg Reimer; 202 pp.

Peters WCH. 1867. Über einige neue oder weniger bekannte Flederthiere. Monatsberichte der Königlichen Preussischen Akademie der Wissenschaften zu Berlin 1866:16–25.

Rainho A, Ferreira DF, Makori B, Bartonjo M, Repas-Gonçalves M, Kirakou S, Maghuwa F, Webala PW, Tomé R. 2023. Guild vertical stratification and drivers of bat foraging in a semi-arid tropical region, Kenya. Biology 12(8):1116. https://doi.org/10.3390/biology12081116

Rohland N, Reich D. 2012. Cost-effective, high-throughput DNA sequencing libraries for multiplexed target capture. Genome Research 22(5):939–946. https://doi.org/10.1101/gr.128124.111

Rosevear DR. 1965. The bats of West Africa. London: British Museum (Natural History); 418 pp.

Salicini I, Ibáñez C, Juste J. 2011. Multilocus phylogeny and species delimitation within the Natterer's bat species complex in the Western Palearctic. Molecular Phylogenetics and Evolution 61(3):888–898. https://doi.org/10.1016/j.ympev.2011.08.010

Schmieder R, Edwards R. 2011. Quality control and preprocessing of metagenomic datasets. Bioinformatics 27(6):863–864. https://doi.org/10.1093/bioinformatics/btr026

Seabra AF. 1898. Sobre um caracter importante para a determinação dos generos e especies dos "Microchiroptera" e lista da especies d'este grupo existantes nas colleçoes de Museo Nacional. Jornal de Sciencias, Mathematicas, Physicas e Naturaes Lisboa, Series 2 5(2):247–258.

Simmons NB. 2005. Chiroptera. In: Wilson DE, Reeder DAM, editors. Mammal species of the world: a taxonomic and geographic reference. 3rd ed. Baltimore (MD, USA): Johns Hopkins University Press; p. 312–529.

Simmons NB, Cirranello AL. 2024. Bat species of the world: a taxonomic and geographic database. Version 1.5. [accessed 16 May 2024]. batnames.org

Srinivasulu C, Srinivasulu A, Srinivasulu B, Jones G. 2019. Integrated approaches to identifying cryptic bat species in areas of high endemism: the case of *Rhinolophus andamanensis* in the Andaman Islands. PLoS One 14(10):e0213562. https://doi.org/10.1371/journal.pone.0213562

StatSoft Inc. 2005. Statistica (data analysis software system), version 7.1. www.statsoft.com

Swynnerton G, Hayman R. 1950. A check list of the land mammals of the Tanganyika Territory and the Zanzibar Protectorate. Journal of the East African Natural History Society 20(6 & 7):274–392.

Taylor PJ, Geiselman C, Kabochi P, Agwanda B, Turner S. 2005. Intraspecific variation in the calls of some African bats (Order Chiroptera). Durban Museum Novitates 30:24–37. https://journals.co.za/doi/pdf/10.10520/AJA0012723X_1887

Taylor PJ, Macdonald A, Goodman SM, Kearney T, Cotterill FPD, Stoffberg S, Monadjem A, Schoeman MC, Guyton J, Naskrecki P, *et al*. 2018. Integrative taxonomy resolves three new cryptic species of small southern African horseshoe bats (*Rhinolophus*). Zoological Journal of the Linnean Society 184(4):1249–1276. https://doi.org/10.1093/zoolinnean/zly024

Taylor PJ, MacDonald A, Goodman SM, Kearney T, Cotterill FPD, Stoffberg S, Monadjem A, Schoeman MC, Guyton J, Naskrecki P, *et al*. 2019. CORRIGENDUM: integrative taxonomy resolves three new cryptic species of small southern African horseshoe bats (*Rhinolophus*). Zoological Journal of the Linnean Society 187(2):535–537. https://doi.org/10.1093/zoolinnean/zlz030

Temminck CJ. 1853. Esquisses zoologiques sur la côte de Guiné. I. Mammifères. Leiden: C. C. Vander Hoek; 256 pp.

Thomas O. 1904. On some small mammals collected by Mr. A. M. Mackilligan in the Eastern Desert of Egypt. Annals & Magazine of Natural History Series 7 14:155–159. https://doi.org/10.1080/03745480409442986

Tu VT, Hassanin A, Görföl T, Arai S, Fukui D, Thanh HT, Son NT, Furey NM, Csorba G. 2017. Integrative taxonomy of the *Rhinolophus macrotis* complex (Chiroptera, Rhinolophidae) in Vietnam and nearby regions. Journal of Zoological Systematics and Evolutionary Research 55(3):177–198. https://doi.org/10.1111/jzs.12169

Van Cakenberghe V, Tungaluna G-CG, Akawa PM, Seamark E, Verheyen E. 2017. The bats of the Congo and of Rwanda and Burundi revisited (Mammalia: Chiroptera). European Journal of Taxonomy 382:1–327. https://doi.org/10.5852/ejt.2017.382

Velazco PM, Gardner AL. 2012. A new species of *Lophostoma* d'Orbigny, 1836 (Chiroptera: Phyllostomidae) from Panama. Journal of Mammalogy 93(2):605–614. https://doi.org/10.1644/11-mamm-a-217.1

Verrett TB, Webala PW, Patterson BD, Dick CW. 2022. Remarkably low host specificity in the bat fly *Penicillidia fulvida* (Diptera: Nycteribiidae) as assessed by mitochondrial COI and nuclear 28S sequence data. Parasites & Vectors 15(1):1–16. https://doi.org/10.1186/s13071-022-05516-z

Webala PW, Oguge NO, Bekele A. 2004. Bat species diversity and distribution in three vegetation communities of Meru National Park, Kenya. African Journal of Ecology 42(3):171–179. https://doi.org/10.1111/j.1365-2028.2004.00505.x